Available online at www.sciencedirect.com
ScienceDirect
Journal of Hazardous Materials 152 (2008) 228–240
Journal of Hazardous Materials
www.elsevier.com/locate/jhazmat

Impact of spatiotemporal fluctuations in airborne chemical concentration on toxic hazard assessment

K.T. Bogen *, F.J. Gouveia

Energy & Environment Directorate, Lawrence Livermore National Laboratory, Livermore, CA 94550, USA

Received 10 June 2006; received in revised form 25 May 2007; accepted 26 June 2007
Available online 5 July 2007

Abstract

Models widely used to assess atmospheric chemical-dispersion hazards for emergency response rely on acute exposure guideline level (AEGL) or similar concentration guidelines to map geographic areas potentially affected by corresponding levels of toxic severity. By ignoring substantial, random variability in concentration over time and space, such standard methods routinely underestimate the size of potentially affected areas. Underestimation due to temporal fluctuation – applicable to chemicals like hydrogen cyanide (HCN) for which peak concentrations best predict acute toxicity – becomes magnified by spatial fluctuation, defined as heterogeneity in average concentration at each location relative to standard-method predictions. The combined impact of spatiotemporal fluctuation on size of assessed threat areas was studied using a statistical-simulation assessment method calibrated to Joint Urban 2003 Oklahoma City field-tracer data. For a hypothetical 60-min urban release scenario involving HCN gas, the stochastic method predicted that lethal/severe effects could occur in an area 18 or 25 times larger than was predicted by standard methods targeted to a 60-min AEGL, assuming wind speeds $\geq$2.0 or $\leq$1.5 m/s, respectively. The underestimation doubled when the standard method was targeted to a 10-min AEGL. Further research and field data are needed for improved stochastic methods to assess spatiotemporal fluctuation effects.

Keywords: Acute toxicity; Atmospheric dispersion; Hydrogen cyanide; Modeling; Risk

1. Introduction

Models widely used to assess atmospheric chemical-dispersion hazards for emergency response purposes use acute exposure guideline level (AEGL) or similar concentration guidelines to map geographic areas potentially affected by corresponding levels of toxic severity. AEGLs are widely applied "threshold" concentrations intended to prevent nearly all effects of specified severity in a general exposed population [1]. However, by focusing on predicted mean concentrations, such standard methods may typically ignore peak-hazard magnifications due to (1) integrated toxic load from releases that differ from any reference averaging times used, (2) temporal concentration fluctuation at each location, and/or (3) spatial fluctuation (or heterogeneity) in the ratios of realized (e.g., measured) toxic loads to corresponding loads modeled by standard methods. For chemicals with acute toxicity that is predicted better by peak than by mean exposure levels, factor 1 (F_1) and factor 2 (F_2) may contribute to potential underestimation of hazard. Factor 3 (F_3) reflects non-modeled (residual) spatial variation in concentration due to non-homogeneous mixing within a dispersion plume, and so by definition also contributes to chemical-independent underestimation of peak levels of hazard. We are not aware of any previous study examining the combined impact of spatial and temporal fluctuations on assessed areas of airborne chemical hazard. Moreover, methods currently available to address all three factors separately may be cumbersome or presently unfeasible to implement, and no method has been proposed to address their joint impact in a realistic urban setting. The aim of the present study was to develop a simple, approximate method to address all three factors for the purpose of protective urban hazard assessment, and to examine the magnitude of difference between its predictions and those produced by current methods for a hypothetical but realistic urban exposure scenario.

Potential impacts of F_1, F_2 and F_3 on estimates of peak hazard follow from the fact that likelihoods of acute chemical toxicity occurrence have been modeled reasonably well for many res-

* Corresponding author. Tel.: +1 510 268 5048; fax: +1 510 268 5099.
E-mail address: kbogen@exponent.com (K.T. Bogen).

0304-3894/$ – see front matter © 2007 Elsevier B.V. All rights reserved.
doi:10.1016/j.jhazmat.2007.06.116

Nomenclature

C	chemical concentration (ppm)
$C(t)$	time-varying C at time t (ppm)
C_T	constant C for exposure duration T (ppm)
C_{T_o}	constant C for exposure duration T_o (ppm)
$\overline{C}_T$, or $\overline{C_T^n}$	TWA value of $C(t)$, or of $[C(t)]^n$, for $0 \le t \le T$ (ppm, or ppm^n)
F_1	hazard magnification factor due to $T/T_o > 1$
F_2	hazard magnification factor due to $C(t)$ fluctuation
F_3	hazard magnification factor due to stochastic spatial heterogeneity in observed relative to modeled values of L_1
$\mathcal{F}_s$	product of terms F_i with i from set $s = \{1,2,3\}$
$\mathcal{F}_s^*$	statistical confidence limit on F_s
H	high wind speeds ($\ge$2.0 m/s)
L	low wind speeds ($\le$1.5 m/s)
L_n	toxic load conditional on C_T and n (ppm^n min[a])
$\mathcal{L}_n$	toxic load conditional on $C(t)$ and n (ppm^n min)
$\mathcal{L}_1^*$	statistical confidence limit on $\mathcal{L}_1$ (ppm min)
M_n	$(F_2)^n$, the nth moment of normalized concentration
n	toxic load exponent
r	sample Pearson product-moment correlation coefficient
R^2	r^2, fraction of explained variance
SED	$\mathcal{L}_1$, or static equivalent dosage (ppm min)
t	time (min)
T	exposure duration (min)
T_o	reference exposure duration (min)
T_{TWA}	averaging period over which TWA estimate of $C(t)$ is made (min)
TWA	time-weighted average

Greek symbols

θ	local wind direction (degrees)
θ'	angular displacement relative to plume-model centerline defined by θ and the source location (degrees)
ρ_n	toxic load ratio $\mathcal{L}_n/L_n$

piratory toxicants using a log-probit model [2] of static toxic load L_n, namely a Gaussian function of a linear transformation of $\log(L_n)$, with L_n defined as

$$L_n = \int_0^T C_T^n \, dt = \overline{C_T^n} T, \quad (1)$$

in which C_T is a constant (static, non-varying) chemical concentration in respired air over time t during an exposure period $0 \le t \le T$, and n is referred to as the toxic load exponent [1,3–6]. The special case in which $n = 1$ is known as Haber's law, and L_1 is sometimes referred to as "dosage" or "integrated dosage". A constant concentration C_T appears in Eq. (1) because experimental exposures used in animal inhalation acute-toxicity experiments that now serve as the empirical basis for most if not all currently available chemical-specific estimates of n typically involved the application of nearly constant chemical concentrations in air (see, e.g., [5] and [7]). By this model, exposure for a reference period T_o, such as $T_o = 10$ min, to any concentration(s) less than or equal to a corresponding guidance (we shall assume AEGL) concentration C_{T_o} is estimated to comprise an exposure sufficiently low to protect against occurrence of a corresponding level of toxic severity in nearly all members of a general exposed population, including relatively susceptible individuals, whereas populations exposed to concentrations $>C_{T_o}$ "could experience" that level of toxic severity ([1], p. 35).

Factor F_1 affects the application of Eq. (1) to assess hazards from exposure to relatively constant concentrations, for exposure periods that happen to differ from those associated with available time-specific AEGL guidelines. If exposure is extended to some fixed duration $T > T_o$, the corresponding maximum constant concentration C_T adequate to protect against the same endpoint is, according to Eq. (1), less than C_T by the factor $(T/T_o)^{1/n}$. Exposure to any constant concentration $C_T > C_{T_o}(T_o/T)^{1/n}$ would be non-protective according to AEGL criteria based on Eq. (1). Hazard underestimation due to F_1 is avoided if the exposure duration of interest is included among available guideline-concentration durations (which for AEGLs are: 10 min, 30 min, 1 h, 4 h and 8 h), and this duration is used as the reference period T_o. However, exposure durations of interest may differ from available durations or from a reference duration applied by default.

Interpolation methods [e.g., [8]] can easily address F_1, but such methods address neither concentration-related temporal fluctuation (F_2) nor spatial variation (F_3), which may separately or jointly pose a potentially greater source of hazard underestimation. Concentration fluctuation has long been well recognized to be a critical consideration in order to prevent gross underestimates of acute hazards posed by respiratory exposure to toxic chemicals [3–6,9–13]. Methods developed to address F_2 [14–16] presently require location-specific estimates of concentration fluctuation that typically are not available, due both to the inherent stochastic nature of fluctuation itself, and to a lack of fluctuation data for large urban areas of greatest practical concern. While available models such as HPAC that implement second-order closure theories do provide a way to estimate F_2 [17,18], such estimates have not yet been validated in relation to corresponding experimental urban dispersion-fluctuation data. Factor F_3 arises from local turbulence that inevitably leads to stochastic heterogeneity in the value of L_n measured or experienced at different locations, above and beyond variation in L_n that may be predicted *ex ante* even by the most sophisticated dispersion forecasting models currently practical to implement. Previous studies of hazard underestimation potentially associated with F_3 have focused on the case of $n = 1$, without regard to other exposure-related sources of potential hazard underestimation [19,20].

As mentioned above, F_1 is properly addressed if AEGLs of the correct exposure duration are available and are applied. Some

[a] F or the purpose of analyzing F_3 variability (Fig. 4), integrated dosage L_1 was normalized by released tracer mass, and expressed in units of s/m^3.

may assume that other factors, F_2 and F_3, typically will only marginally affect hazard assessment for atmospherically dispersed chemicals, and/or that such potential effects are already accounted for by "uncertainty" or safety factors routinely incorporated into AEGLs. However, such safety factors may vary tremendously from chemical to chemical, and can be quite low for some important toxic industrial chemicals (e.g., a factor of just eight in the case of hydrogen cyanide) [21]. AEGL safety factors are not derived with reference to exposure-related factors such as F_2 or F_3, nor is the relationship between exposure modeling issues and the intended application of AEGLs even mentioned in underlying AEGL-methodology documentation [1]. When AEGLs are applied without modification to assess airborne chemical hazards under realistic conditions, factors F_2 and F_3 are likely to reduce the effective degree of protection relative to stated AEGL goals of protecting nearly all of any general exposed population against specified levels of toxic severity. No previous study has explored such joint effects, either quantitatively or qualitatively.

Here we develop and illustrate an approximate method to address F_1, F_2 and F_3 jointly for the purpose of protective urban hazard assessment. This method incorporates the first reported estimates of F_2 and F_3 ever obtained directly from a large, urban field-study data set. After briefly describing the urban tracer data used to characterize F_2 and F_3, Section 2 presents the proposed analytic approach, and then explains how the empirical urban data were used to parameterize this approach. Section 3 summarizes the data analysis, its incorporation into the proposed approach, and an illustrative application of the resulting approach to a hypothetical 60-min release of hydrogen cyanide (HCN) gas in a major US urban area. Sections 4 and 5 then consider limitations of key assumptions used, study implications, and conclusions.

2. Methods

2.1. Urban tracer data

Collection of very detailed tracer dispersion data for the largest US urban areas (like that modeled in the present study, as described below) began only fairly recently, preceded by smaller "joint urban" studies of this type done in Salt Lake City and in Oklahoma City. Tracer data for Oklahoma City, Oklahoma, obtained during the Joint Urban 2003 study (JU2003) [22–24] were selected to estimate the quantitative impact of all three factors considered, because this study currently provides the most comprehensive set of fast-response-time measures required to characterize F_2 under realistic urban conditions. This extensive field experiment included over a hundred scientists measuring airflow, tracer concentration, and other variables pertinent to urban dispersion. (For a detailed description of JU2003, see: http://ju2003.pnl.gov/.) During JU2003, atmospheric concentrations of the inert tracer gas, sulfur hexafluoride (SF_6), and associated airflow were measured by instruments including an array of geographically fixed field devices used during 10 intensive observation periods (IOPs), with additional airflow measures taken over a 35-day period. Each 12-h IOP featured two or three separate 30-min tracer releases, and several puff releases. Data for a total of 214 30-min time series, included in data previously modeled and analyzed by Gouveia [24], were further analyzed in the present study.

Source locations, release times, measured wind speeds and directions (which varied for the different IOPs), and corresponding instrumentation were summarized previously [22–24]. Briefly, the tracer data comprise JU2003 tracer concentrations measured by Lawrence Livermore National Laboratory (LLNL), the Volpe National Transportation Systems Center (Volpe) of the US Department of Transportation, and the National Oceanic and Atmospheric Administration (NOAA). The LLNL and Volpe samplers were all within 350 m of the source, and a few within 10 m. The NOAA samplers (Programmable Integrating Gas Samplers, PIGS) were placed at street intersections within the urban center (NOAA grid), and in arcs roughly 1, 2, and 4 km from the source (NOAA arcs). The Volpe, grid and arc samplers all collected integrated sample data at a rate of $\leq$0.001 Hz. Two types of high-speed LLNL detectors were deployed: Blue Box (programmable bag samplers) with a sample-measure rate of $\leq$0.04 Hz, and Miran (infrared spectrometric) samplers each with a 2.23 l chamber volume measuring SF_6 at 1 Hz with throughput driven by a 45-l/min pump (providing mean effectively independent sampling periods of $\sim$3 s); each Miran sampler was configured either as a point sampler, or as a line sampler drawing air through $\sim$15 m of outstretched perforated tubing. Raw concentration data in ppb by volume were analyzed directly to characterize F_2; to characterize F_3, concentration data ($\mu g/m^3$) were integrated and divided by total microgram SF_6 released to obtain corresponding normalized dosage (L_1, defined by Eq. (2) below, but expressed in $\mu g\ s/m^3$ per μg SF_6 released, i.e., in s/m^3).

Average values of local wind direction (θ) and wind speed were measured at $\geq$1 Hz during each 30-min release, either by a Young Model 05103 Wind Monitor placed at elevations ranging from 1 to 3 m in a Portable Weather Information Display System station located near each release source (applied to model all LLNL, Volpe and NOAA grid concentrations, except those from six Park Avenue releases for which modeling was based on wind measures made using a Metek USA-1 ultrasonic anemometer placed at 8.5 m elevation on the Arizona State University tower), or by a Young Model 81000 ultrasonic anemometer placed at the lowest (7.8-m) level of an LLNL crane situated downwind approximately midway between each release source and the NOAA arc samplers (applied to model all NOAA arc concentrations).

2.2. Analytic model

For scenarios involving exposure at a fixed location for a duration T to a fluctuating concentration $C(t)$ at all times t, $0 \leq t \leq T$, the corresponding dynamic toxic load (or "dosement" [9]) is defined as

$$\mathcal{L}_n = \rho_n L_n = \int_0^T [C(t)]^n \, dt = \overline{C_T^n} T \quad (2)$$

where overbar and T-subscript together denote time-weighted average (TWA) over duration T, where L_n was defined in Eq.

(1) in terms of a constant concentration $C_T = \overline{C_T}$, and where in Eq. (2) conditioning on $C(t)$ realized at each fixed location is tacit. The fluctuating concentration $C(t)$ is understood to represent a series of k discrete mean values each estimated over an averaging-time period $T_{TWA} = T/k$, with k chosen to ensure that T_{TWA} is the minimum biologically relevant response period over which concentration fluctuation can increase toxicity relative to that induced by exposure to a corresponding average concentration [9,14].

The "enhancing factor" or "toxic load ratio" [9,15] ρ_n that appears in Eq. (2) is defined as the ratio of any given dynamic toxic load to its corresponding static toxic load, which ratio is (as shown below) convenient to re-express as follows in terms of the three factors defined above:

$$\rho_n = \frac{\mathcal{L}_n}{L_n} = (F_1 F_2 F_3)^n = (F_1 F_3)^n M_n \tag{3}$$

In Eq. (3), M_n denotes the nth sample moment of location-specific normalized concentration $C(t) = \overline{C}_T$ during the interval $0 \le t \le T$, and is defined as

$$M_n = (F_2)^n = \frac{\overline{C_T^n}}{(\overline{C}_T)^n} \tag{4}$$

In particular, $E(M_2) = I^2 + 1$ where E is the expectation operator and I is often referred to as the "concentration intensity" (i.e., coefficient of variation, or standard deviation divided by the mean) of $C(t)$.

From Eqs. (1) and (2) and the factor definitions given above, $F_1 = (T/T_o)^{1/n}$ (a constant, conditional on T_o and n), F_2 models normalized temporal variation in toxic load, and F_3 models residual stochastic spatial variation in toxic load with $E(F_3) = 1$ if the dispersion model used is unbiased. F_3 was assumed to have a median equal to 1, corresponding to emergency conditions under which bias-reducing optimization against real-time concentration data is not feasible. In the absence of any theoretical or empirical basis for assuming that F_2 and F_3 should be correlated, these factors were assumed to be statistically independent. This assumption was tested using LLNL Miran data from the JU2003 study.

Empirical M_n behavior was a focus of the concentration fluctuation experiments (CONFLUX) project conducted on salt flats at the US Army Dugway Proving Ground in northwestern Utah, in which an array of many very fast-response detectors was used to measure propylene tracer gas continuously released for a period of 30–35 min in each of a large series of open-terrain, atmospheric dispersion studies covering a very wide range of atmospheric conditions and release configurations [25]. Note these continuous-release durations were about the same as those used in the JU2003 study. Studies of CONFLUX data have established that $\log(M_n)$ is very nearly linearly proportional to $[(n-1)\log(M_2)]$, in accordance with expectations based on a variety of (e.g., gamma, clipped gamma, clipped normal and exponential) probability models found to provide reasonably good characterizations of variation in normalized $C(t)$ observed in a wide range of CONFLUX data [10,12,13,15]. The exponential model yields the particularly convenient expectation [13,15] that

$$M_n \approx \Gamma(n+1)\left(\frac{M_2}{2}\right)^{n-1} \tag{5}$$

which by Eq. (4) implies that the factor F_2 can be approximated by

$$F_2 = \Gamma(n+1)^{1/n}\left(\frac{M_2}{2}\right)^{1-1/n}, \tag{6}$$

that is, by a monotonic function of n and of location-specific sample moment M_2. Data from the JU2003 urban tracer-release study revealed substantial measured variance in M_2, very little of which could be explained by downwind or crosswind distance from release sources (see Section 3.1). Therefore, M_2 values in urban locations were modeled as random samples from distributions estimated from M_2 measures made using JU2003 data.

We assume, as above, that a specified (reference) AEGL defines a threshold value of constant chemical concentration C_{T_o}, above which a general population exposed by inhalation for duration T_o "could experience" a specified level of toxic severity. The current practice of limiting actual population exposures of duration T_o to a modeled static dosage $L_1 = C_{T_o} T_o$ may not be protective, because a non-negligible fraction of the exposed population will inevitably incur a larger (by definition, non-protective) dosage to an extent determined jointly by the magnitudes of F_3 variation and of the slope of log-probit dose-response for the chemical of concern. Due to factors F_1 and F_2, even less protection is afforded if the same dosage limit $C_{T_o} T_o$ is applied over a period $T \ge T_o$ during which exposure occurs to a dynamic, fluctuating concentration $C(t)$ with a TWA concentration of C_T—unless the value of C_T adopted in this case is sufficiently less than C_{T_o} so as to guarantee the same level of protection as that intended by the AEGL C_{T_o} limit under uniform exposure conditions. For a generalized dynamic exposure scenario, it is thus convenient to derive the corresponding dynamic toxic load $\mathcal{L}_1$ – which shall be referred to as "static equivalent dosage" (SED) – as follows based on definitions given in Eqs. (2)–(4):

$$\mathcal{L}_1 = C_T T = \left[\frac{C_{T_o}}{F_1 F_2 F_3}\right] T = \left(\frac{C_{T_o}}{\mathcal{F}_{\{1,2,3\}}}\right) T \tag{7}$$

where $\mathcal{F}_s = \prod_{i \in s} \mathcal{F}_i$ and s is any one of the seven possible combinations containing at least one of the indices $\{1,2,3\}$. A lower confidence limit $\mathcal{L}_1^*$ on $\mathcal{L}_1$ is obtained by substituting the corresponding upper confidence limit $\mathcal{F}_s^*$ for $\mathcal{F}_s$ in Eq. (7), noting that $\mathcal{F}_1^* = \mathcal{F}_1 =$ a constant. The SED* value obtained by using a sufficiently high (e.g., 2-tail 95%) upper confidence limit $\mathcal{F}_s^*$ on $\mathcal{F}_s$ by definition provides a level of protection comparable to that intended by the reference AEGL concentration C_{T_o}. Note that the product $\mathcal{L}_1 \mathcal{F}_s$ is simply a convenient way to denote $\mathcal{L}_1$ conditional on the absence of each factor involved in $\mathcal{F}_s$, which also is the case for $\mathcal{L}_1^*$ and $\mathcal{F}_s^*$. The SED measures described are all expressed in simple units (e.g., total integrated ppm min), so calculations based on them can easily be incorporated into a wide variety of modeling tools cur-

rently available to assess atmospherically dispersed chemical hazards.

2.3. Data analysis and model application

To model variability in F_2 arising from that in M_2, characterizations and comparisons were done on fluctuation levels exhibited in above-background sets of JU2003 concentration data obtained only from high-speed (1-Hz) LLNL Miran detectors, up to nine of which were used simultaneously in all IOPs during each 30-min release. The concentration data were first pre-processed to delete pre- and post-release-pulse data involving below-background concentration data. In-pulse data sets were then combined and classified by sampler type, by time block (day versus night), and by urban-center wind speed divided into two approximately equally frequent categories – low (L) for speeds $\leq$1.5 m/s, and high (H) for speeds $\geq$2.0 m/s – which excluded intermediate speeds simply to create a more meaningful dichotomy in the wind variable analyzed.

To model F_3 variability, characterizations and comparisons were done using scores $Z_{i,k} = (\delta_{i,k} - \mu_k)/\sigma_k$ obtained for the relative residuals $\delta_{i,k} = \log_{10}[(\text{measured } \mathcal{L}_1)/(\text{modeled } \mathcal{L}_1)]|\{i,k\}$ corresponding to each ith measure made by detector type k (with k = LLNL, Volpe, NOAA grid, or NOAA arc), and where μ_k and σ_k are the sample mean (i.e., bias) and standard deviation of $\delta_{i,k}$ for each k. Corresponding estimates of μ_k, σ_k and modeled dosage were obtained for the present illustrative study using (for convenience) a simple Gaussian-plume model previously described [24]. Conditional on each known experimental tracer release mass, the Gaussian model was conditioned only on average values of local wind direction (θ) and wind speed measured as described above (Section 2.1). The plume model was not otherwise optimized to fit additional data obtained for each set of tracer measurements, such as angular displacement (θ') relative to the plume-model centerline that was defined by θ and the source location.

Thus obtained, F_3 was used to characterize bias-adjusted spatial error in integrated dosages (or TWA concentrations) predicted by the Gaussian-plume model used, rather than the LODI dispersion model (applied for toxicity hazard assessment as described below) for which a complete set of JU2003 modeling results are not yet available. The Gaussian-plume model used is less complex (and, at least for larger-scale applications, less accurate) than the particle-tracking LODI model. However, representing bias-adjusted magnitudes of difference between measured and modeled concentrations, F_3 by definition is not affected by any difference in relative model accuracy. Both the Gaussian and (currently implemented) LODI models are designed to predict only ensemble mean concentrations within an evolving plume, rather than F_3-type heterogeneity (i.e., variance) comprising "random" deviations between actual (or measured) concentrations and mean values predicted at any location by either model. If a single, common underlying mixing mechanism were the cause of all such characteristic (e.g., ground-level) spatial variability in concentration that occurs in dispersion plumes realized under similar driving-source and meteorological conditions, then a measured F_3 error distribution under those conditions could have a fairly simple stochastic form. The present study includes a test of this prediction.

Spatial dosage heterogeneity (F_3) was also analyzed by release period (day versus night) and by angular displacement (θ') relative to the plume-model centerline. To prevent random effects due to sensitivity limits and to poorly modeled lateral or upwind mixing processes, these analyses were done using only modeled and measured values $\mathcal{L}_1 \geq 10^{-7}$ s/m^3 at detector locations for which $|\theta'| \leq 45^\circ$. The F_2- and F_3-related data were characterized using 2-tail t-tests (or, as applicable, Welch's t-tests) to assess differences in normalized means [26], Bartlett's chi-square tests to assess corresponding variance homogeneity [27], Kolmogorov 2- or 1-sample or (or, in comparisons involving >500 samples) corresponding asymptotic Smirnov tests to test for difference between sample cumulative mass functions (cmfs) or between a theoretical cumulative distribution function (cdf) and a sample cmf, respectively [28,29], and chi-square tests to test for difference between a sample cmf and an estimated cdf. To obtain 10-min AEGL-based $\mathcal{L}_1^*$ values for the illustrative application described below, $\mathcal{F}_s$ variability was modeled using Monte Carlo methods to obtain 5000 sample vectors of F_i for $i \in s$, each modeled as described above, together with an iterative optimization procedure to assure zero Pearson correlations $\pm < 10^{-5}$, noting that F_1 is a constant, and two types of F_2 were calculated: one each for low (L) and high (H) wind conditions, respectively. These calculations were all performed using Mathematica 5.0® and related RiskQ software [30,31].

The method described above to assess the impact of factors F_1, F_2 and F_3 was applied to a hypothetical scenario involving a 60-min, continuous ground-level release of 1000 kg of HCN gas (0.278 kg/s) at a fixed location during July of 2005 in a major US urban area, with wind from the SW at 2 m/s measured at 10 m, and other meteorological conditions typical of the specific location used for the hypothetical release. In this application, a toxic load exponent of $n = 2.6$ was assumed for lethal or severe HCN effects [7, vol. 2]. Atmospheric HCN dispersion was modeled using the LLNL LODI model, which includes a suite of meteorological and dispersion models (http://narac.llnl.gov/modeling.php). Meteorological input data on mean wind, pressure, precipitation, temperature, and turbulence variables are generated using a variety of interpolation methods and atmospheric parameterizations, including non-divergent wind fields produced by an adjustment procedure based on the variational principle and finite-element discretization [32]. The LODI dispersion model solves the 3D advection-diffusion equation using a Lagrangian stochastic, Monte Carlo method to simulate the processes of mean wind advection, turbulent diffusion, first-order chemical reactions, wet deposition, gravitational settling, dry deposition, buoyant/momentum plume rise, and (for non-chemical applications) radioactive decay and production as well as bio-agent degradation. The LODI model is linked at LLNL to GIS and other databases providing topography, geographical data, demographic data, chemical-biological-nuclear agent properties and health risk indices, real-time meteorological observational data, and global and mesoscale forecast model predictions [33,34].

3. Results

3.1. Concentration statistics

A total of 214 sets of 1-Hz measures of above-background dispersed-tracer concentration C were measured during and/or after each corresponding 30-min release by LLNL detectors arrayed in Oklahoma City during the JU2003 study (Fig. 1). The mean (± 1 standard error of the mean) of plume-passage durations T detected at all locations was 34.1 ± 0.4 min. The arithmetic mean autocorrelation value for (211) data sets with $T \geq 10$ min drops from 1 to 0.80, 0.50, 0.34, 0.16 and 0.06 after lags of approximately 6, 17, 30, 60 and 120 s, respectively. To assess the effect of averaging-time period T_{TWA} on M_2 calculation, corresponding arithmetic mean and upper-bound values of M_2 for these 211 data sets were estimated from $C(t)$ over corresponding durations T using a range of different averaging-time periods T_{TWA}, including that used by the Miran detectors (sampling at 1 Hz, $T_{TWA} = 1$ s). These means (and corresponding upper 2-tail 95% confidence limits) were found to decrease from 100% of those estimated using $T_{TWA} = 1$ s, to 91%, 88%, 82%, 68% and 52% (and to 97%, 91%, 86%, 75% and 63%) at T_{TWA} values of 15, 20, 30, 60 and 120 s, respectively. Therefore, mean and upper-bound M_2 calculations from 1 Hz measures of $C(t)$ in these data sets would (due to the substantial autocorreleation noted) be reduced only slightly (by ~10% or less) if M_2 were instead calculated using longer averaging times ≤ 20 s.

Associated empirical measures of M_n versus M_2 obtained for n values ranging from 3 to 5 were found to be reasonably consistent with corresponding relationships expected according to approximation (6) under the assumption that $C(t)$ is exponentially distributed (Fig. 2). Sample cmfs obtained for M_2 measures made by LLNL Miran point samplers during periods when urban wind speed was low ($\leq$1.5 m/s), versus high ($\geq$2 m/s), are shown in Fig. 3, together with corresponding gamma cdfs. The gamma parameters $\{\alpha, \beta\} = \{6.63, 0.0837\}$ were fit by the method of moments for low wind (L) data, and $\{3.53, 0.0837\}$ for high wind (H) data, where $\{\alpha, \beta\} = \{\mu^2/\sigma^2, \sigma^2/\mu\}$ using sample mean (μ) and variance (σ^2) estimates obtained for each wind speed range. The F_2 characterization was restricted to data from 64 versus 41 point (and not from 30 versus 54 line) LLNL Miran samplers operating under L versus H conditions, respectively, because

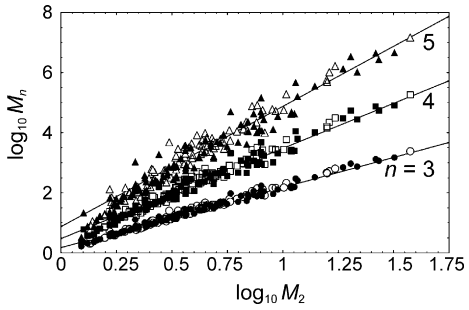

Fig. 2. Log–log plot of measured values (points) of the nth vs. the second normalized moments of $C(t)$, from 214 sets of in-pulse, above-background concentration data on tracer dispersion obtained by LLNL detectors arrayed in Oklahoma City during the JU2003 study, compared to corresponding expected relationships (solid curves) assuming $C(t)$ has an exponential distribution. Solid vs. open points denote measures during low ($\leq$1.5 m/s) vs. high ($\geq$2.0 m/s) urban wind speeds, respectively.

the L-specific M_2-cmfs were significantly different ($p = 0.030$), the line sampler data having a ~20% smaller mean ($p = 0.040$) and about half the variance of the point sampler data. The H-specific M_2-cmfs for point-sampler data did not differ substantially ($p = 0.089$). The point-sampler L- and H-specific cmfs (Fig. 3) differ significantly ($p = 0.017$), and to approximately the same extent as mentioned above for the comparison of L-specific point versus line sampler data; the gamma distributions shown are good fits to these corresponding cmfs ($p > 0.30$). A similar comparison indicated no significant differences ($p > 0.05$) between 124 daytime and 90 nighttime M_2 measures, regardless of sampler type. Using 115 sets of data restricted to Mirans located downwind of each release source for which $|\theta'| \leq 45°$, M_2 measures were found to have small, negative, non-significant correlations ($R^2 \leq 0.024$, $p > 0.10$) with downwind and cross-wind distances from the release source.

A comparison of $\log_{10}$-transformed values of (bias-adjusted) measured values with corresponding modeled values of total integrated dosage ($\mathcal{L}_1$, in s/m^3) in Oklahoma City during the JU2003 study (Fig. 4) indicates general consistency in the magnitude of residual variability for measures made by combined LLNL and Volpe detectors compared to those made by more distantly positioned NOAA grid and arc detectors. Corresponding residual statistics are summarized for each data set in Table 1, and the relation between $|\theta'|$ and the variance of the residu-

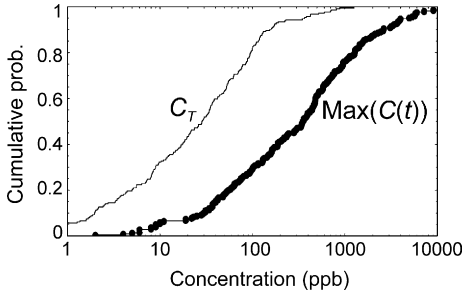

Fig. 1. Cumulative distributions of TWA concentration, C_T, and maximum concentration, Max($C(t)$), from 214 sets of in-pulse, above-background concentration data on tracer dispersion obtained by LLNL detectors arrayed in Oklahoma City during the JU2003 study.

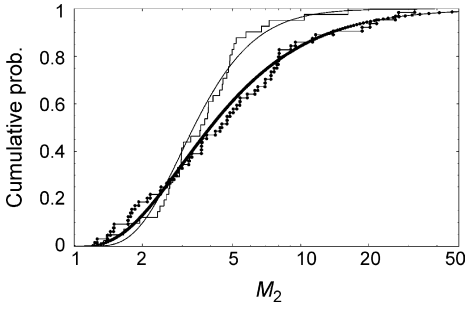

Fig. 3. Cumulative distributions (cmfs) of (unitless) M_2 values measured by LLNL Miran point samplers during periods when urban wind speed was low ($\leq$1.5 m/s, bold step function, L) vs. high ($\geq$2 m/s, light step function, H), together with corresponding fitted gamma distributions.

Table 1
Measured JU2003 concentrations vs. non-optimized Gaussian model predictions[a]

Detector-specific data set (k)	n	Release time	Bias[b], μ_k	Standard deviation, σ_k	Geometric standard deviation, GSD = $10\sigma_k$
LLNL point	97	All	0.341	0.612	4.09
LLNL line	52	All	0.226	0.684	4.83
Volpe	139	All	0.248	0.586	3.85
	211	Day	0.252	0.628	4.25
LLNL + Volpe	77	Night	0.336	0.568	3.69
	288	All	0.275	0.613	4.10
	289	Day	0.155	0.431	3.35
NOAA grid	109	Night	0.326	0.658	4.55
	398	All	0.201	0.508	3.22
	151	Day	0.146	0.421	2.64
NOAA arc	104	Night	0.434	0.526	3.35
	255	All	0.263	0.487	3.07
LLNL + NOAA	941	All	0.241	0.538	3.45

[a] The number, sample mean and sample standard deviation are listed for residual concentrations $\delta_{i,k} = \log_{10}$(measured tracer concentration, ppmv) − $\log_{10}$(predicted tracer concentration, ppmv) for each kth data set, using measured and corresponding Gaussian-plume-model predicted values described in Section 2.

[b] Model bias could be reduced by optimizing, e.g., wind direction in the Gaussian plume models used [24]. The measured wind direction at the release site assumed in each of those models fairly accurately predicted the distribution of corresponding normalized concentration realized for some of the releases, but for others a systematic shift of such distributions away from their predicted centerlines indicated that unmodeled plume curvature was likely to have occurred during these releases [24; cf. Fig. 5 in that study and related discussion therein]. Such shifts may largely explain the estimated bias terms listed.

als is summarized in Table 2. LLNL and Volpe data subsets were combined because no significant differences were found among corresponding sample $\delta_{i,k}$ means or variances, respectively (also found true when NOAA grid versus arc data were compared). The sample variance of NOAA-data $\log_{10}$ residuals ($\sim 0.50^2$) is slightly but significantly less than that ($\sim 0.61^2$) of combined $\log_{10}$ residuals of measures made by the more closely positioned LLNL/Volpe detectors ($p < 0.001$). While the variance of LLNL + Volpe data residuals for the nighttime releases does not differ significantly from the daytime-residual variance ($p = 0.29$) shown in Table 1, the grid- and arc-specific variances of NOAA-data residuals for nighttime releases listed in that table are significantly greater than the corresponding daytime-residual variances ($p < 10^{-5}$). Notably, only one of the six sets of NOAA or combined-LLNL residuals categorized by release time has a geometric standard deviation (GSD) that is <3 (Table 1).

The variance of residuals $\delta_{i,k}$ is clearly positively correlated with the absolute angle $|\theta'|$ measuring relative deviation from the non-optimized plume-model centerline (Table 2). The GSD of measured-to-modeled $\mathcal{L}_1$ ratios corresponding to these residuals increases from just below 3 near the centerline, to almost 5 toward the upper (45°) boundary placed on $|\theta'|$ for the purpose of characterizing F_3 (Table 2). In contrast, using 115 sets of data restricted to Mirans located downwind of each release source for which $|\theta'| \leq 45°$, M_2 measures were found to be virtually uncorrelated with $|\theta'|$ ($R^2 = 0.060$, $p = 0.69$).

The simple Gaussian model accounts for $R^2 = 65.5\%$ of the variance of the combined set of 941 bias-adjusted $\mathcal{L}_1$ measures plotted in Fig. 4 in relation to corresponding modeled values of $\mathcal{L}_1$. As noted above, $|\theta'|$ significantly predicts the variance of corresponding residuals, which by definition is unaffected by bias-adjustment. However, adding either θ' or $|\theta'|$ to $\log_{10}$(modeled $\mathcal{L}_1$) as a linear predictor of $\log_{10}$(measured $\mathcal{L}_1$) did not significantly increase the explained residual variance R^2 ($F_{1,938} \leq 1.11$, $p > 0.29$). The distribution of corresponding $Z_{i,k}$ scores is ~N(0,1) ($p = 0.18$), and is consistent with an approximately common, underlying lognormal distribution of normalized spatial modeling errors with ~95% of observations within a factor of about 10 of the (median) Gaussian model prediction. Similar results were obtained when spatial variabil-

Table 2
Relation between $|\theta'|$ and heterogeneity in the ratio (ρ) of measured-to-modeled dosage ($\mathcal{L}_1$) at different Oklahoma City locations in the JU2003 study[a]

Range of angle θ' from source to detector relative to plume-model centerline	Mean value of $\lvert\theta'\rvert$ (°)	Number of measures, m	SD(δ)	Var (δ)[b]	GSD (ρ)	Ratio[c] of upper 95% CL to median value of ρ
$\lvert\theta'\rvert \leq 9°$	3.6	267	0.459	0.210	2.88	7.9
$9° < \lvert\theta'\rvert \leq 18°$	13.8	250	0.485	0.236	3.06	8.9
$18° < \lvert\theta'\rvert \leq 27°$	21.8	151	0.559	0.313	3.62	12.5
$27° < \lvert\theta'\rvert \leq 36°$	31.0	181	0.591	0.349	3.90	14.4
$36° < \lvert\theta'\rvert$	40.4	92	0.680	0.463	4.79	21.5

[a] $\delta = \log_{10}(\rho)$ where ρ = (measured $\mathcal{L}_1$)/(modeled $\mathcal{L}_1$), based on m total measures for which $\mathcal{L}_1 \geq 10^{-7}$ s/m^3 and $|\theta'| \leq 45°$. SD = standard deviation, Var = variance, GSD = geometric SD

[b] The listed variances differ significantly by Bartlett's test ($p = 1.5 \times 10^{-6}$).

[c] Ratio (q) of upper 2-tail confidence limit (CL) on ρ to the median value of ρ under the assumption that ρ is lognormally distributed, i.e., that $q = \text{GSD}(\rho)^{1.96}$.

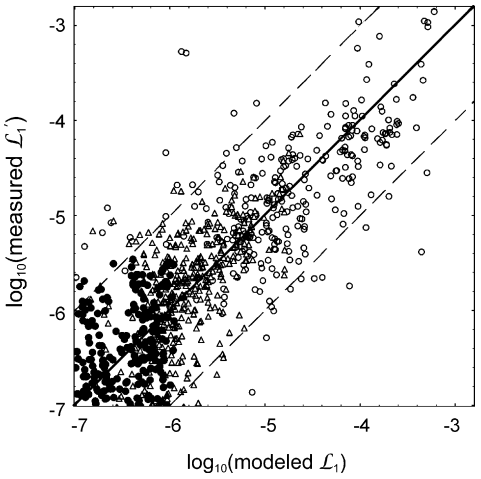

Fig. 4. Comparison of bias-adjusted measures ($\mathcal{L}_1'$) and corresponding modeled values of total integrated dosage $\mathcal{L}_1$ in Oklahoma City during the JU2003 study, conditional on $\mathcal{L}_1 \geq 10^{-7}$ s/m^3 and $|\theta'| \leq 45°$, in which m data values were collected by detector type k: combined LLNL and Volpe detectors (◯, $m = 288$, $k = 1$), NOAA grid detectors (△, $m = 398$, $k = 2$), and NOAA arc detectors (●, $m = 255$, $k = 3$). Each ith bias-adjusted measure from detector type k indicated on the Y-axis is defined as $\mathcal{L}_1' = 10^{-\mu_k}(\mathcal{L}_1|\{i,k\})$, using corresponding estimated biases μ_k listed in Table 1.

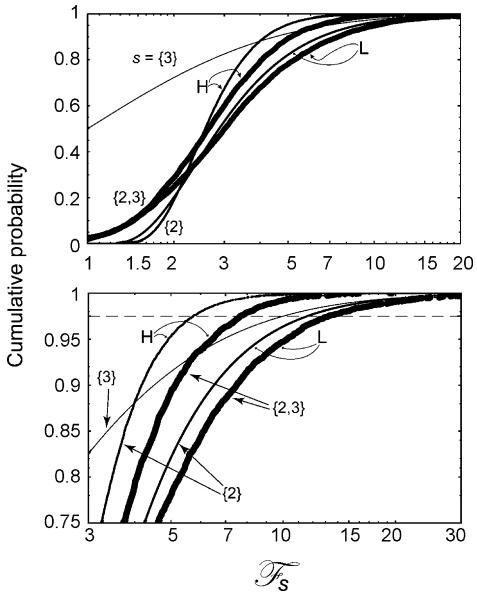

Fig. 5. Cumulative distributions (cdfs) of (unitless) $\mathcal{F}_s$ for the indicated values of s (top and bottom plots): {2} (two medium-width curves), {3} (single thin curve), and {2,3} (two thick curves), during periods when urban wind speed is low (≤1.5 m/s, L) vs. high (≥2 m/s, H). Greater detail (bottom plot) highlights each curve's upper 2-tail 95% confidence limit ($\mathcal{F}_s$ value at which that curve crosses the horizontal dashed line). The $s = \{2\}$ and $s = \{2,3\}$ pair of curves that correspond to low-wind (L) conditions (e.g., the rightmost pair of curves in bottom plot) reflect greater variability than those that correspond to high-wind (H) conditions.

ity data from were analyzed by wind speed category (L versus H). Overall, the normalized spatial variability data are thus consistent with random, approximately lognormal variability with 95% of observations within a factor of approximately 10 of the (median) Gaussian model prediction. Thus, F_3 was modeled as a lognormal distribution with a median of 1, a geometric standard deviation of exp(1.175) = 3.238, and an upper 2-tail 95% confidence limit of $F_3^* = 10$. Note this limit, $F_3^* = 10$, corresponds to a ratio defined identically to that for which values (ranging from 7.9 to 21.5) are listed in the right-most column of Table 2 in relation to corresponding values of $|\theta'|$. Table 2 implies that F_3^* could more accurately be modeled as a function of $|\theta'|$, in a way that would (relative to setting $F_3^* = 10$ independent of $|\theta'|$) reduce its impact along the plume centerline by ~20%, but magnify this impact ≥2-fold for $|\theta'| \geq 45°$. However, the simpler approach of modeling F_3 as lognormal with $F_3^* = 10$ was used to implement the illustration discussed in Section 3.2.

Using the 115 sets of data referred to above obtained by Mirans located downwind of each release source for which $|\theta'| \leq 45°$, M_2 measures at these sites were found to have only a marginally significant, small positive correlation ($R^2 = 0.046$, $p = 0.021$) with corresponding bias-adjusted residuals (or with corresponding scores $Z_{i,k}$) upon which the lognormal model assumed for F_3 was based. Corresponding correlations between F_2 (calculated using approximation 6, using $n = 2.6$ or $n = 3$) and F_3 were even smaller ($R^2 \leq 0.045$, $p \geq 0.022$). Because only relative low-speed detectors were used from hundreds to thousands of meters downwind in the JU2003 study, F_2 could not be estimated and consequently no assessment of potential correlation between F_2 and F_3 could be made at those positions.

Distributions and upper limits on $\mathcal{F}_s$ corresponding to F_2 (under assumed low and high wind speed conditions) and/or F_3 as defined above are shown in Fig. 5.

3.2. Application to hypothetical chemical-release scenario

Table 3 summarizes results obtained when the proposed approach was applied to derive $\mathcal{L}_1^*$ values for HCN. Ten- and 60-min AEGL assessments for the hypothetical HCN-release scenario described in Section 2 are shown in Fig. 6a and b. The 10-min AEGL plot (Fig. 6a) shows three LODI-generated contours along values of $L_1 = C_{T_o} \times T_o$, where $T = T_o = 10$ min, and where C_{T_o} = each of the three, severity-level-specific 10-min AEGL concentration values for HCN. The impact of factors F_1, F_2 and F_3 on predicted threat zones for this scenario was calculated simply by having LODI use corresponding SED-related estimators (involving $\mathcal{L}_1^*$) instead of L_1 to generate the plotted AEGL-specific contours. Corresponding results of combining the illustrative application of the proposed approach with LODI assessments for the same scenario are shown in Fig. 6c and d for $\mathcal{L}_1^* \mathcal{F}_3^*$ under high versus low wind speed conditions, respectively, and in Fig. 6e and f for $\mathcal{L}_1^*$ under high versus low wind speed conditions, respectively. Corresponding LODI estimates of affected areas and maximum affected population (assuming ambient exposures, without mitigation due to indoor air turnover) are shown in each panel of Fig. 6 for the three AEGL toxic severity levels (1 = mild, 2 = serious, 3 = severe). Compared to the default 10-min AEGL approach (Fig. 6a), application of the proposed method in this illustration under low wind conditions (Fig. 6f) resulted in magnification of estimated areas affected by factors of approximately {18, 36, 51} for AEGL severity levels {1, 2, 3}, respectively, and magnification of estimated maximum population affected by factors of approximately {6.9, 12, 22}

Table 3
10- and 60-min AEGLs for HCN, and corresponding SED values[a]

	10-min AEGL-3 (ppm) (a[b])	60-min AEGL-3 (ppm) (b)	$\mathcal{L}_1^*\mathcal{F}_3^*$ high[b] (ppm min) (c)	$\mathcal{L}_1^*\mathcal{F}_3^*$ low[b] (ppm min) (d)	$\mathcal{L}_1^*$ high[b] (ppm min) (e)	$\mathcal{L}_1^*$ low[b] (ppm min) (f)
AEGL severity level						
1 (mild)	2.5	2.0	21	10	16	9.1
2 (serious)	17	7.1	130	73	63	48
3 (lethal or severe)	27	15	180	94	120	79

[a] SED = static equivalent dosage.
[b] Dispersion model cases (a–f) correspond to panel letters that appear in Fig. 6. high = higher wind speeds (≥2.0 m/s); low = lower wind speeds (≤1.5 m/s).

for AEGL severity levels {1, 2, 3}, respectively. The resulting magnification factors were thus substantial (five of the six factors are > 10), and these factors increase (nearly linearly) with increasing AEGL severity level. This magnification was due primarily to F_2 and F_3 (temporal and spatial fluctuation), rather than to F_1 (AEGL averaging time), since areas potentially affected at each severity level associated with 60-min AEGLs were only about twofold greater than corresponding areas associated with 10-min AEGLs (Fig. 6b versus a).

4. Discussion

The results obtained indicate that application of the proposed methods, which account more realistically for spatial and temporal concentration fluctuations than do current methods, could result in substantially greater levels of assessed hazard at each of three levels of toxic severity considered. In particular, the potentially severely or lethally affected area estimated by a 10-min (or 60-min) AEGL approach was shown, for the hypothetical release scenario considered under low wind conditions, to be about 50 (or 25) times less than that estimated using the proposed methods to account more realistically for the combined impact of spatial and temporal concentration fluctuations. The results obtained are clearly preliminary because only limited (JU2003) data were available upon which to base a model accounting for temporal and spatial concentration fluctuations in a realistic urban setting. Analysis of urban dispersion data from additional urban settings will be required to develop a more general basis for improved modeling of the impact of temporal and spatial concentration fluctuations in urban settings.

The following six important additional issues were not addressed in the proposed modeling approach illustrated, which jointly may render the proposed approximate approach slightly or moderately biased either toward overprediction or toward underprediction of airborne chemical hazards.

(1) Downwind and crosswind distance were observed to explain very little of the variance in concentration fluctuation intensity observed in that subset of JU2003 data obtained using relatively high-speed detectors (see Section 3.1), in contrast to previous indications that these factors may predict some aspects of fluctuation exhibited in tracer-release studies conducted in open-field or rectangular-obstacle-array conditions in an otherwise rural environment [10,25,35]. Concentration fluctuation intensity has been theorized as well as observed in continuous-release studies to diminish with downwind distance X, albeit in a nonlinear way, e.g., modeled by Ma et al. [36] as $M_2 = (a + b/X)^2 + 1$ for $X > 1$ with fitted parameters a and b, and as $M_2 \propto X^{1/2}$ by Yee et al. [25] who concluded that "the alternative interpretation that [our observed] fluctuation intensities achieve near constancy in level with downwind distance within the turbulent convective regime of cloud development cannot be ruled out, given the experimental scatter in our data". Previous studies have thus concluded that relative centerline concentration fluctuation intensity has "considerable scatter" and "remains significant at large distances from the source, particularly for ground-level sources" [37], and "is seen to change very slowly with downwind distance" [25]. Omission of this factor from the proposed approach to model F_2 may thus result in a small to moderate degree of hazard overprediction. More detailed study of urban continuous-release data is required to assess the relative importance of this omitted factor.

(2) In contrast, relative concentration fluctuation intensity has been observed in continuous-release studies to increase supra-linearly (e.g., approximately exponentially) with increasing crosswind distance from the plume centerline [10,25]. While this relationship was not evident from the present analysis of near-field JU2003 data, insofar as M_2 and $|\theta'|$ were found to be nearly independent (Section 3.1), this issue could not be explored for data collected farther downwind in this study because the sampling rates used at those positions were too slow to measure M_2 at biologically relevant intervals. Potential off-centerline magnification of M_2 unaddressed by the proposed approximate method implies that it may underpredict increased hazard due to temporal concentration fluctuations. Again, more detailed studies of urban continuous-release data are required to assess the relative importance of this omitted factor.

(3) For the present study, concentration fluctuation intensity was measured using an effective averaging period of ~3 s. A greater sampling period on the order of 5–30 s likely better reflects the biologically relevant averaging time for respiratory toxicants such as HCN [9,14]. Use of a greater averaging period is expected to reduce corresponding calculated concentration fluctuation intensities, according to empirically verified theoretical expectations [38,39]. However, the JU2003 concentration data were found to be sufficiently autocorrelated to ensure that this effect was minimal for averaging periods within the range of those that are biologically relevant. Omission of this factor thus in this

case implies only a slight overprediction of increased hazard due to temporal concentration fluctuations. It must also be borne in mind that results from this study are applicable only to urban areas, given that concentration fluctuation intensity measures made in continuous-release field experiments involving a plume dispersing through a regular array of obstacles (intended to model urban/suburban conditions) were observed to be "generally a factor of between 2 and 5 smaller" than those measured in otherwise similar open-terrain plume experiments [35].

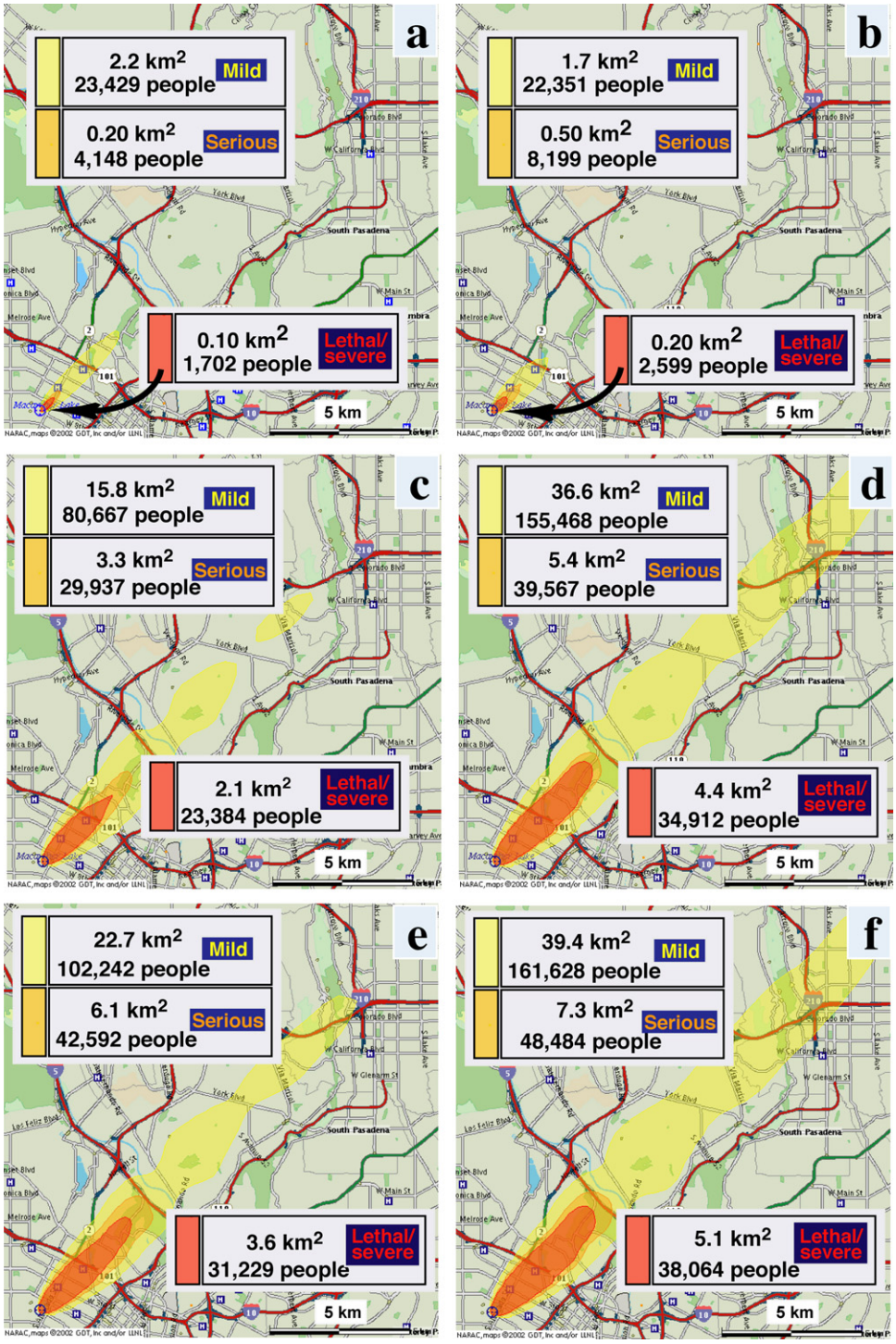

Fig. 6. LODI predictions of atmospheric dispersion and hazard level posed by a hypothetical ground release of 1000 kg of hydrogen cyanide (HCN) gas over a 1 h period in an urban California area. Assessments made using the current method for 10- and 60-min AEGLs (panels a and b, top left and right, respectively) are compared to corresponding assessments made using the proposed modified method for $\mathcal{L}_1^*\mathcal{F}_3^*$ under high vs. low wind speed conditions (panels c and d, respectively), and for $\mathcal{L}_1^*$ under high vs. low wind speed conditions (panels e and f, respectively). LODI estimates of areas and maximum potentially affected populations corresponding to each of three AEGL toxic severity levels (1 = mild, 2 = serious, 3 = severe) are shown in each panel.

(4) The approximate method used to characterize F_3, reflecting non-modeled (residual) spatial variation in dosage (time-integrated concentration) due to non-homogeneous mixing, relies on a bias-adjusted comparison of one model's dispersion predictions to observations. Such a characterization of residual error can be model-dependent only in ways that reflect the complexity of the physics incorporated in the model, the numerical error in the model, as well as the initial and boundary conditions supplied to the model and other model-dependent factors. In the present study, F_3 was characterized using a Gaussian-plume model applied to JU2003 data (Fig. 4), for simplicity without regard to off-centerline crosswind position indexed by $|\theta'|$ (the effect of ignoring $|\theta'|$ was discussed in Section 3.1, in relation to Table 2). To illustrate potential implications, this simplistic characterization was mapped onto dispersion results obtained for a much larger US urban location using a different model (LODI). The approximate lognormality of the distribution of combined JU2003 adjusted residuals obtained in this study is consistent with a common underlying (e.g., chaotic microscale turbulence) mechanism likely to generate the type of stochastic spatial heterogeneity in time-integrated concentrations denoted by F_3. Interestingly, a stochastic multifractal model describes a lognormally distributed (spatial or temporal) process if its multifractal (Levy-distribution) index α approaches 2 within its bounds $0 \leq \alpha \leq 2$, and multifractal-model-fitted α values between 1.6 and 1.8 appear to be the norm for analyzed meteorological data, including experimental data on atmospheric dispersion of SF_6 tracer gas [40]. Because both the Gaussian and LODI models used in this study are designed to predict only ensemble mean plume concentrations, future LODI analysis of JU2003 data may not substantially alter the F_3 characterization applied to the hypothetical scenario considered here. Such an expectation is supported by the similarity in magnitudes of residual dosage-related variation observed when data obtained from 0.1 to 6 km downwind during 18 1-h SF_6 tracer-release experiments in the JU2003 study done in Oklahoma City were compared to corresponding prediction made by six different dispersion models, including five urban-adapted Gaussian-type models and one empirical "one-line" urban model [41]. Although the predicted-versus-observed scatter plots from that study show somewhat less relative variation than that indicated for F_3 by Fig. 4 in the present study, the former study involved far fewer measures, and these were all plotted in terms of maximum 1-h average concentration rather than dosage ($\mathcal{L}_1$) [41]. In future studies, it will be important to continue to compare the performance of different modeling approaches to characterize F_3.

(5) In simulating the product (F_2 F_3), the stochastic factors F_3 and F_3 were assumed to be statistically independent, in accordance with our analysis of applicable data available from the JU2003 study in Oklahoma City indicating little if any correlation between these factors within several hundred meters downwind. Assuming a positive correlation between these factors would necessarily have increased both the expected value and variance of their product, and hence would have magnified the chemical threat zones estimated for our illustrative HCN-release scenario. Improved estimates of correlation between F_2 and F_3 require new field data from urban tracer-release studies specifically designed to address this question over a broad range of downwind distances.

(6) Our analysis did not account explicitly for either sampling/measurement error pertaining to sample moments of concentration, which can be substantial [42–44]. Neither did we account explicitly for uncertainty associated with approximation (5) used to predict urban realizations of M_n conditional on corresponding realizations of M_2 as evident in Fig. 2, even for relatively small n with $n > 2$. Incorporating these additional uncertainties into our approach would magnify the chemical threat zones estimated for our illustrative HCN-release scenario.

Future studies should be encouraged to address these limitations of this first effort to characterize and address the magnitude of combined spatiotemporal fluctuation impacts on urban chemical threat zone estimation. Much progress has been made in developing and applying computational fluid dynamics (CFD) and large-eddy simulation (LES) models to more realistically predict complicated atmospheric dispersion patterns that arise in urban environments [45–47]. Some of the most realistic, numerically intensive CFD models were recently shown to provide reasonably good and consistent predictions of concentration over time in a tracer-release study conducted in Manhattan [45]. However, all of these models were characterized as being "currently too slow to be used for real-time emergency response" in urban areas at least several km^2 in size [45]. Although it is very likely that such models will eventually be able to predict irregularities and magnitudes of spatiotemporal fluctuation over large-scale urban areas like those exhibited in JU2003 data (e.g., on a statistical basis using multiple realizations), no such capability has yet been validated. When this ability does become available, some or perhaps even most of the variability associated with the factors F_2 and F_3 we address will become subsumed in the dispersion model used, and thus will not need to be modeled statistically as proposed here. The important point is that the underlying variability associated with these factors, as reflected in JU2003 data and in future urban tracer-release studies designed to address them, will need to be reflected one way or another in chemical threat assessment models. The present study has shown that substantial empirical joint variability associated with these factors is not reflected in atmospheric chemical-dispersion models now used for real-time emergency response, and consequently that greater prudence is required to protect public health in the event of an urban chemical release than is now widely assumed.

A strength of the present analysis – its characterization of F_3 based on multiple dispersion data sets obtained over the course of an urban tracer-release experiment – will be important to retain in future analyses. Additionally, F_3 is expected to vary not just with low- versus high-wind-speeds, but perhaps more predictably with atmospheric stability. Subsequent analyses of F_3 will ideally distinguish between the non-homogenous mix-

ing anticipated in the stable (often nocturnal) atmosphere and that which occurs in the unstable (often daytime) atmosphere. Although the built-up centers of urban areas with tall buildings often exhibit neutral stability regardless of the time of day [48], densely populated suburban areas [49] experience a wide range of stability conditions, and thus F_3 would be expected to change dramatically in those areas.

Finally, it is important to emphasize that the comparative chemical hazard assessments reported here using different modeling assumptions represent hypothetical protective (not predictive) assessments done only for illustrative purposes. As such, the estimated sizes of maximum potentially affected populations given in Fig. 6 do not in any way represent casualty estimates, but rather are merely estimated populations located within the indicated (cumulative) zones. These population sizes do not reflect any protective effect of building occupancy (indoor sheltering), nor do they integrate casualty likelihood using quantitative dose–response information. Explicit consideration of sheltering in our study would merely change the magnitude of populations potentially affected, not the magnitude of relative difference between affected-population estimates obtained using our approach versus the more traditional approach, conditional on the building occupancy assumptions used.

5. Conclusions

Approximate methods examined here to account for concentration fluctuation differ from previously considered methods to assess the likelihood of toxic impact from atmospherically dispersed chemicals [9,14–16,50], in three key ways. The new methods proposed here: (1) apply specifically to an urban setting, (2) address both spatial and temporal (i.e., not just temporal) variation in concentration, and (3) facilitate environmental health protection decisions using conservative (upper-bound) criteria consistent with the application of AEGL methodology to identify geographic zones that include or exclude substantial likelihood of the occurrence of toxic effects at specified levels of severity. A key limitation of the proposed approach arises from the fact that item (3) just listed – effectiveness for environmental health protection – implies that this method cannot be applied reliably to problems that require environmental health triage or trade-offs that may arise in complex exposure scenarios involving multiple chemical agents or a mixture of chemical and other harmful agents or processes [21]. To address triage problems, the proposed methods would need to be adapted to focus on expected, rather than upper-bound, levels of casualty, using an integrated probabilistic approach along lines previously described [9,14,15,21].

For the hypothetical 60-min HCN-release scenario analyzed, this study showed that explicit consideration of temporal and spatial variability in modeled concentrations caused about a 20-fold increase in the predicted size of the potentially lethally/seriously affected area, compared to the standard method applied. This underestimation by the standard method was ~2-fold greater when this method was targeted to a 10-min rather than 60-min AEGL. Despite its limitations, this study illustrates a statistical-simulation method that more realistically addresses spatiotemporal concentration variability than current standard methods. Further research and field data are needed for improved stochastic methods to assess spatiotemporal fluctuation effects.

Acknowledgements

We are grateful for LODI assessment runs conducted for this study by Fernando Aluzzi, and to Gayle Sugiyama, Julie Lundquist, Don Ermak and an anonymous reviewer for suggestions on earlier drafts of this manuscript. This work was performed under auspices of the US Department of Energy by University of California, Lawrence Livermore National Laboratory (LLNL) under Contract W-7405-Eng-48, with support from the LLNL National Atmospheric Release Advisory Program and Carbon Management Program.

References

[1] National Research Council (NRC), Standing Operating Procedures for Developing Acute Exposure Levels for Hazardous Chemicals, National Academies Press, Washington, DC, 2001. [AEGLs are the guidelines of first choice recommended currently by U.S. federal regulatory agencies involved in emergency response; see U.S. Environmental Protection Agency Acute Exposure Guideline Program (http://www.epa.gov/oppt/aegl/); U.S. Department of Energy Order 151.1C (Comprehensive Emergency Management Systems Objectives) §4.a(14)(d)2, 2 Nov. 2005 (http://www.directives.doe.gov/pdfs/doe/doetext/neword/151/o1511c.html).].

[2] D.J. Finney, Probit Analysis, Cambridge University Press, London, UK, 1971.

[3] R.M.J. Withers, F.P. Lees, The assessment of major hazards: The lethal toxicity of chlorine. Part 1, Review of information on toxicity, J. Hazard. Mater. 12 (1985) 231–282.

[4] R.M.J. Withers, F.P. Lees, The assessment of major hazards: The lethal toxicity of chlorine. Part 2, Model of toxicity to man, J. Hazard. Mater. 12 (1985) 283–302.

[5] W.F. ten Berge, A. Zwart, L.M. Appelman, Concentration-time mortality response relationship of irritant and systemically acting vapours and gases, J. Hazard. Mater. 13 (1986) 301–309.

[6] F.J. Miller, P.M. Schlosser, D.B. Janszen, Haber's rule: a special case in a family of curves relating concentration and duration of exposure to a fixed level of response for a given endpoint, Toxicology 149 (2000) 21–34.

[7] National Research Council (NRC), Acute Exposure Guideline Levels for Selected Airborne Chemicals, vol. 1–4. National Academies Press, Washington, DC, 2000, 2002, 2003, 2004.

[8] S.A. Stage, Determination of acute exposure guideline levels in a dispersion model, J. Air Waste Manag. Assoc. 54 (2004) 49–59.

[9] D.J. Ride, An assessment of the effects of fluctuations on the severity of poisoning by toxic vapours, J. Hazard. Mater. 9 (1984) 235–240.

[10] E. Yee, R. Chan, P.R. Kosteniuk, G.M. Chandler, C.A. Biltoft, J.F. Bowers, Experimental measurements of concentration fluctuations and scales in a dispersing plume in the atmospheric surface layer obtained using a very fast response concentration detector, J. Appl. Meteorol. 33 (1994) 996–1016.

[11] D.M. Lewis, Monte Carlo estimate of dosages of gases dispersing in the atmosphere, Environmetrics 8 (1997) 629–650.

[12] E. Yee, R. Chan, A simple model for the probability density function of concentration fluctuations in atmospheric plumes, Atmos. Environ. 31 (1997) 991–1002.

[13] E. Yee, R. Chan, Comments on "Relationships between higher moments of concentration and of dose in turbulent dispersion", Boundary-Layer Meteorol. 82 (1997) 341–351.

[14] T.L. Hilderman, S.E. Hrudey, D.J. Wilson, A model for effective toxic load from fluctuating gas concentrations, J. Hazard. Mater. A 64 (1999) 115–134.
[15] E. Yee, An impact-effect mathematical model incorporating the influence of exposures to fluctuating concentrations in a dispersing plume of pollutant in the atmosphere, J. Expos. Anal. Environ. Epidemiol. 9 (1999) 300–311.
[16] S.J. Dyster, D.J. Thomson, C.A. McHugh, D.J. Carruthers, Turbulent fluctuations and their use in estimating compliance with standards and in model evaluation, Int. J. Environ. Pollut. 16 (2001) 57–68.
[17] U.S. Defense Threat Reduction Agency (DTRA), The Hazard Prediction and Assessment Capability (HPAC) user's guide Version 4.0.3, HPAC-UGUIDE-02-U-RAC0 (Prepared for the U.S. DTRA by Science Applications International Corporation, 602 pp.), DTRA, Alexandria, VA, 2001.
[18] S. Warner, N. Platt, J.F. Heagy, Comparisons of transport and dispersion model predictions of the URBAN 2000 field experiment, J. Appl. Meteorol. 43 (2004) 829–846.
[19] J.S. Irwin, 2008. Modeling air quality pollutant impacts, EORASAP (European Assoc. for the Sci. of Air Pollut.) Newsletter 40 (Dec. 2000) http://meteo.bg/EURASAP/40/paper1.html. (2000).
[20] E. Sajo, An estimate of spatial uncertainty of mean concentrations predicted by Gaussian dispersion models, Health Phys. 85 (2003) 174–183.
[21] K.T. Bogen, Risk analysis for environmental health triage, Risk Anal. 25 (2005) 1085–1095.
[22] K.J. Allwine, K. Clawson, M.J. Leach, D. Burrows, R. Wayson, J. Flaherty, E. Allwine, Urban dispersion processes investigated during the Joint Urban 2003 Study in Oklahoma City, Proceedings of the Fifth Conference on Urban Environment, American Meteorological Society (AMS) Conference, 23–26 August 2004, Vancouver, BC, 2004.
[23] K. Clawson, R.G. Carter, D.J. Lacroix, N.F. Hukari, K.J. Allwine, Joint Urban 2003 vertical SF6 real-time analyzer and time-integrated sampler data characteristics, Proceedings of the Fifth Conference on Urban Environment, American Meteorological Society (AMS) Conference, 23–26 August 2004, Vancouver, BC, 2004.
[24] F.J. Gouveia, Gaussian modeling of tracer concentrations during the Joint Urban 2003 experiment, Proceedings of the Fifth Symposium on the Urban Environment, American Meteorological Society (AMS) Conference, 23–26 August 2004, Vancouver, BC, 2004.
[25] E. Yee, P.R. Kosteniuk, J.F. Bowers, A study of concentration fluctuations in instantaneous clouds dispersing in the atmospheric surface layer for relative turbulent diffusion: basic descriptive statistics, Boundary-Layer Meteorol. 87 (1998) 409–457.
[26] M. Kendall, A. Stuart, The Advanced Theory of Statistics, Vol. 2: Inference and Relationship, 4th ed., MacMillan Publishing Co, NY, 1979, pp. 159–160.
[27] G. Snedecor, W.G. Cochran, Statistical Methods, 8th ed., Iowa State University Press, Ames, IA, 1989, p. 251.
[28] R.R. Wilcox, Some practical reasons for reconsidering the Kolmolgorov-Smirnov test, Br. J. Math. Stat. Psychol. 50 (1997) 9–20.
[29] P.J. Kim, On the exact and approximate sampling distribution of the two sample Kolmogorov-Smirnov criterion Dmn, $m \leq n$, J. Am. Statist. Assoc. 64 (1969) 1625–1637.
[30] S. Wolfram, Mathematica Book, 4th ed., Cambridge University Press, Cambridge, UK, 1999.
[31] K.T. Bogen, RiskQ 4.2: An Interactive Approach to Probability, Uncertainty and Statistics for use with Mathematica®, UCRL-MA-110232 Rev. 3. Lawrence Livermore National Laboratory, Livermore, CA, 2002.
[32] G. Sugiyama, S.T. Chan, A new meteorological data assimilation model for real-time emergency response, in: Proceedings of the 10th Joint Conference on the Applications of Air Pollution Meteorology, 11–16 January 1998, Phoenix, AZ, Am. Meteorol. Soc., Boston, MA, 1998, pp. 285–289.
[33] D.L. Ermak, J.S. Nasstrom, A Lagrangian stochastic diffusion method for inhomogeneous turbulence, Atmos. Environ. 34 (2000) 1059–1068.
[34] J.S. Nasstrom, G. Sugiyama, J.M. Leone Jr., D.L. Ermak, A real-time atmospheric dispersion modeling system, in: Proceedings of the 11th Joint Conference on the Applications of Air Pollution Meteorology, Long Beach, CA, 9–14 January 2000. American Meteorological Society, Boston, MA, 2000.
[35] E. Yee, C.A. Biltoft, Concentration fluctuation measurements in a plume dispersing through a regular array of obstacles, Boundary-Layer Meteorol. 111 (2004) 363–415.
[36] Y. Ma, Z. Boybeyi, S. Hanna, K. Chayantrakom, Plume dispersion from the MVP filed experiment. Analysis of surface concentration and its fluctuations, Atmos. Environ. 39 (2005) 3039–3054.
[37] D.M. Lewis, A simple model of concentration fluctuations in neutrally buoyant clouds, Boundary-Layer Meteorol. 90 (1999) 117–153.
[38] A. Venkatram, The expected deviation of observed concentrations from predicted ensemble means, Atmos. Environ. 13 (1979) 1547–1549.
[39] S.R. Hanna, The exponential probability density function and concentration fluctuations in smoke plumes, Boundary-Layer Meteorol. 29 (1984) 361–375.
[40] D. Finn, B. Lamb, M.Y. Leclere, S. Lovejoy, S. Peckhold, D. Schertzer, Multifractal analysis of line-source plume concentration fluctuations in surface-layer flows, J. Appl. Meteorol. 40 (2001) 229–245.
[41] S.R. Hanna, P. Fabian, J.C. Chang, A. Venkatram, R. Britter, M. Neophytou, D. Brook, Use of Urban 2000 Field data to determine whether there are significant differences between the performance measures of several urban dispersion models, Am. Meteorol. Soc. Proceedings of the Fifth Conference on Urban Environment, 23–26 August 2004, Vancouver, BC, Canada, 2004, paper 7.3.
[42] V.G. Alexseyev, Accuracy of experimental determination of higher-order moments of time series, Eng. Cybern. (1970) 1195–1201.
[43] R.M. Tuggle, The relationship between TLV-TWA compliance and TLV-STEL compliance, Appl. Occup. Environ. Hyg. 15 (2000) 380–386.
[44] G.A. Korn, Random-Process Simulation and Measurements, McGraw-Hill Book Co, New York, NY, 1966, pp. 95–99.
[45] S.R. Hanna, M.J. Brown, F.E. Camelli, S.T. Chan, W.J. Coirier, O.R. Hansen, A.H. Huber, S. Kim, R.M. Reynolds, Detailed simulations of atmospheric flow and dispersion in downtown Manhattan: An application of five computational fluid dynamics models, Bull. Am. Meteorol. Soc. 87 (2006) 1713–1726.
[46] C. Chan, M. Leach, A validation of FEM3MP with Joint URBAN 2003 data, J. Appl. Meteorol. Climatol., in press.
[47] J. Lundquist, S. Chan, Consequences of urban stability conditions for computational fluid dynamics simulations of urban simulations, J. Appl. Meteorol. Climatol., in press.
[48] J.K. Lundquist, J. Shinn, F. Gouveia, Observations of the turbulent kinetic energy dissipation rate in the urban environment, in: Proceedings of the Symposium on Planning, Nowcasting, and Forecasting in the Urban Zone. American Meteorological Society Symposium, 10–15 January 2004, Seattle, WA, 2004.
[49] J.C. Weil, R.S. Sheu, R. Frehlich, M.L. Jensen, Dispersion during nighttime light-wind conditions near the Pentagon, in: Proceedings of the 9th Annual George Mason University Conference on Atmospheric Transport and Dispersion Modeling, 18–20 July 2005, Fairfax, VA, 2005.
[50] National Research Council (NRC), Tracking and Predicting the Atmospheric Dispersion of Hazardous Materials Releases: Implications for Homeland Security, National Academies Press, Washington, DC, 2005.